NMR-based metabonomics study on liver and kidney tissues from type 2 diabetic mice

S. Cai[1], J. Y. Yang[2], J. Xu[1], J. Dong[1], and Z. Chen[1]

[1]Department of Physics, Xiamen University, Xiamen, Fujian, China, People's Republic of, [2]Department of Biomedical Sciences, Xiamen University, Xiamen, Fujian, China, People's Republic of

Introduction

NMR-based metabonomics [1] has been widely used in many areas including disease diagnosis and drug development. Presently, the studies are mainly focused on biofluids, such as urine, serum and saliva [2]. In contrast to biofluids, biological tissues have the advantage of determining organ-specific metabolic fingerprints. In this report, high-resolution magic-angle spinning (HRMAS) ^{1}H NMR coupled with principal component analysis (PCA) is utilized to investigate the liver and kidney tissues of model mice for type 2 diabetes mellitus (T2DM).

Materials and Methods

Seven male C57BLKS/J-db/db mice were used as T2DM models while six male C56BLKS/J-db/m mice were used as control. The animal room was under controlled condition (temperature, humidity, and a 12-hour light-dark cycle) and the animals were provided with food and water *at libitum*. Animals were sacrificed by cervical dislocation at the age of 8 weeks and their left lateral lobes of liver and cortical sections of kidneys were dissected, immediately snap-frozen in liquid nitrogen and stored at -80 °C until NMR experiments.

Tissue samples (20 ± 2 mg) were flushed with sufficient D_2O and then placed in a 4 mm ZrO_2 rotor. D_2O was added to the samples to provide field-lock signal, together with 3 mM DSS (2,2-dimethyl-2-silapentane-5-sulfonic acid) as chemical shift reference. ^{1}H MAS spectra of the tissues were acquired at 293K on Varian NMR System 500 MHz spectrometer. Experimental sequence was the conventional pre-saturation for water suppression incorporated with a spin echo (CPMG) train, and the spin rate of the rotor was 2 kHz. All NMR spectra were phased, baseline corrected and segmented into regions of δ 0.04 width in the region of δ 0.48 ~ 4.48. The spectral segments were scaled to total integrated area of each spectrum to account for the differences in concentration.

Results and Discussion

Liver and kidney tissues were targeted since they are easy to obtain and their spectroscopic profilings have been reported [3,4]. More importantly, they are two sites critical for metabolism and vulnerable to high glucose-induced damage and diabetic complications. Therefore the identification of characteristic metabolites in sick liver and kidney tissues would be of great help for exploring the pathogenesis of diabetes.

The metabonomics differences of liver tissues between the diabetic and control groups are visible in Fig. 1(a), where the data points of each class are well-clustered and the separation between two classes is good. The contributions of different regions of the spectra to the classification are illustrated in the PC loading plot in Fig. 1(b). It suggests that the separation is mainly attributed to the triglyceride, trimethylamine-*N*-oxide (TMAO), phosphocholine (PC), glycerophosphocholine (GPC) and choline. Compared to the control mice, the triglyceride signals increase acutely in the liver tissues of the db/db mice, indicating evident hepatic steatosis. This is probably due to insufficient insulin actions by the age of 8 weeks which lead to abnormal regulation of transcriptional expression and activities of many important metabolic nuclear receptors. The glucose and lipid metabolism is affected so that the synthesis of triglycerides is increased while its degradation might be down-regulated, resulting in significant accumulation in the liver. Besides, the levels of PC/GPC, TMAO and choline which are either intermediates or derivatives of methylamine metabolism decline obviously. One reason for the significant hepatic reduction of these methylamines in the db/db mice might be related to osmotic regulation.

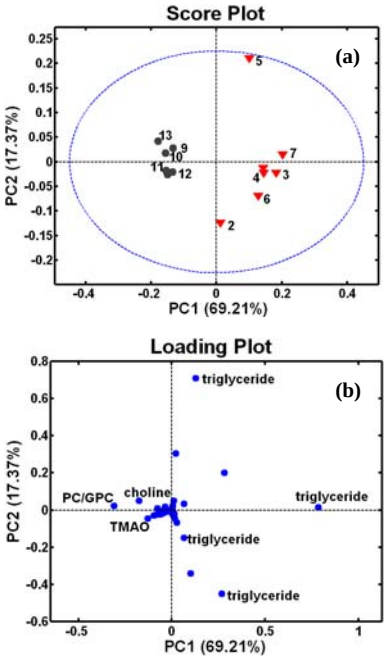

Fig. 1 PC score plot (a) and loading plot (b) (PC1 vs PC2) of ^{1}H MAS spectra of liver tissues from db/db (1-7,▼) and db/m (8-13,●) mice.

In db/db mice, overt diabetic nephropathy normally begins at the age of around 16 weeks. However, there should be a series of molecular events happened much earlier before evident diabetic nephropathy. It is therefore interesting to look for early metabolic markers in the renal metabolic profiles. The score plot from the autoscale method (Fig. 2(a)) displays a reasonable clustering among different groups. The separation of the two classes is not so clear as in the score plot of liver tissues, indicating relatively less organ lesions. When the meancenter method was used, the data points belonging to different classes are mixed together in the resulting score plot (Fig. 7(b)). This may be explained by the properties of datasets processed by different pretreatment method. The autoscale method adjusts the differences in concentration between different metabolites, thus more sensitive in detecting low concentration metabolites under minor symptoms of renal lesions in 8-weeks-old db/db mice.

Conclusion

In this study, high resolution ^{1}H MAS NMR spectroscopy integrated with multivariate statistical analysis has been applied to investigate the liver and kidney tissues of db/db mice at early diabetic stage. The results show clear differences in liver tissues between 8-weeks-old diabetic and control mice in metabonomics traits whereas only minor metabonomics separation is observed in kidney tissues. Although *ex vivo* NMR technique only detect final metabolites, it has a potential in discovering the primary aetiological factor of diabetes mellitus, providing an insight into the mechanism of disease and organ lesions.

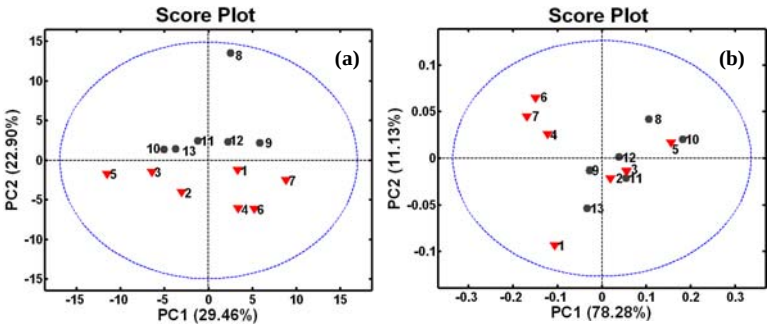

Fig. 2 PC score plots (PC1 vs PC2) of ^{1}H MAS spectra pretreated with autoscale (a) and meancenter (b) methods from kidney tissues of db/db (1-7,▼) and db/m (8-13,●) mice.

Acknowledgements

This work was partially supported by the NNSF of China under Grants 10875101 and 30770490, and Key Project of Health and Science and Technology of Xiamen under Grant 3502Z20051027.

References

[1] Nicholson JK, et al. Xenobiotica 29 (1999) 1181-1189.
[2] Griffin JL, et al. Curr Opin Chem Biol 7 (2003) 648-654.
[3] Wu HF, et al. Anal Biochem 339 (2005) 242-248.
[4] Martinez GB, et al. NMR Biomed 19 (2006) 90-100.